Turkish Journal of Civil Engineering, 2025, 27-51, Paper 819, ***Research Article***

Seismic Performance of Chevron-Braced Steel Buildings with Beam Yielding Mechanism Using FEMA P695 Methodology

Serdar SELAMET[1*]
Ahmet Alperen ORGEV[2]

ABSTRACT

Current seismic design provisions for chevron-braced frames require that the chevron beams resist the unbalanced force due to simultaneous brace buckling and tensile yielding, leading to deep heavy chevron beams. Results of large-scale chevron braced frames have demonstrated that allowing limited chevron beam yielding reduces this unbalanced force and is not detrimental to the lateral resistance of chevron-braced buildings. This proposed design reduces the size of beams in chevron-braced frames. This study evaluates the seismic performance of 3-story and 9-story prototype buildings with the proposed design. The novelty of this research lies in applying FEMA P695 seismic provisions for performance and collapse risk assessment, and ASCE 41 modeling parameters and acceptance criteria for nonlinear brace, beam, and column elements in the numerical building models. Results indicate compelling evidence that the proposed design with reduced sized chevron beams offer seismic performance comparable to frames designed according to current AISC provisions. The collapse risk in 50 years remains within acceptable limit of 2% for both designs. Additionally, the proposed design also provides a more economical solution, reducing structural weight of the braced-frame by up to 8%, thus enhancing the applicability in practice for chevron-braced steel buildings.

Keywords: Chevron-braced frames, SCBF, seismic response, steel braced frames, FEMA P695.

Note:
- This paper was received on July 24, 2024 and accepted for publication by the Editorial Board on May 6, 2025.
- Discussions on this paper will be accepted by January 31, 2026.
- https://doi.org/10.18400/tjce.1521408

1 Bogazici University, Department of Civil Engineering, Istanbul, Türkiye
Stanford University, Department of Civil and Environmental Engineering, Stanford, CA 94305, USA
serdar.selamet@bogazici.edu.tr - sselamet@stanford.edu - https://orcid.org/0000-0001-9444-470X

2 Bogazici University, Department of Civil Engineering, Istanbul, Türkiye
Istanbul Technical University, Department of Civil Engineering, Istanbul, Türkiye
ahmet.orgev@bogazici.edu.tr - alperen.orgev@itu.edu.tr - https://orcid.org/0000-0003-3603-7246

* Corresponding author

1. INTRODUCTION

Concentrically braced frames (CBFs) have historically been a preferred structural system for seismic steel design because they provide high strength and stiffness. Special concentrically braced frames (SCBFs) are commonly used as lateral-load-resisting systems in seismic regions. Chevron (or inverted V-braced) SCBFs are used to accommodate architectural openings, such as doors, windows, mechanical openings and elevators [1]. Zheng et al. [2] analyzed seismic performance of different chevron braced frames, revealing that variations in brace configurations significantly affect their energy dissipation and load-carrying capacities. More specifically, the research conducted by Li et al. [3] highlighted the importance of optimizing beam design in chevron braced frames to improve their overall seismic performance.

Current seismic US and European provisions for SCBFs require chevron beams to resist the unbalanced brace forces due to post-buckling compressive strength deterioration and full tensile yielding of the braces [4,5]. The brace members create large axial force and bending moment demand in beams, which results in relatively deep and heavier sections compared to the beam cross sections in alternative bracing systems [5,6]. While chevron CBFs were common prior to about 1988, these lateral resistive systems are rarely used today because of the heavy chevron beam strength requirement, which reduces the economy and efficiency of the system. Recent experimental and numerical research proposed that a new design for chevron-braced frames, denoted as proposed design herein [5,6]. The proposed design uses lighter chevron beams as an additional yielding mechanism, where the tension brace force is assumed to be equal to the expected compressive capacity at buckling of the compression brace thereby reducing the unbalanced load on the beam. Experimental studies showed this assumption holds true and sufficient ductility (i.e., story drifts more than 3%) is achieved by a plastic mechanism consisting of brace buckling and chevron beam flexural yielding [6]. Previous research has shown that numerical models of 2D (planar) braced frames using the nonlinear structural analysis software Perform 3D [7] capture the overall load-deformation behavior prior to brace fracture with reasonable accuracy [8,9,10].

The study validates a new criterion for design (i.e. braced-frame design with reduced sized chevron beams) and assesses the seismic and collapse risk performance of the proposed design by 3-story and 9-story chevron-braced buildings, which were selected as representative archetypes for low-rise and mid-rise structures commonly encountered in seismic regions. It is acknowledged that a broader range of building configurations could provide additional insights. However, this selection aligns with the methodology prescribed in FEMA P695, “Quantification of Building Seismic Performance Factors” [11], which allows the use of targeted archetypes to evaluate performance factors under realistic conditions. By analyzing these two archetypes, the study captures a broad range of structural responses, including the differing dynamic behaviors of shorter, stiffer buildings and taller, more flexible structures. The performance assessment is based on the framework using FEMA P695. The nonlinear modeling parameters and acceptance criteria are based on ASCE 41, “Seismic Evaluation and Retrofit of Existing Buildings” [12], which are the industry standards for seismic evaluation and retrofit of existing buildings. The methodology includes incremental nonlinear dynamic analysis of the structural models, supported by a ground motion scaling process used to normalize and scale the selected records to match the seismic

hazard levels at the fundamental period of the building. Fragility and hazard curve estimations are then conducted based on the results of the dynamic analyses.

2. METHODOLOGY

AISC 341-16, "Seismic Provisions for Structural Steel Buildings" [13], requires capacity-based design for SCBFs and the current seismic specifications state that: (1) the braces should resist the factored lateral loads while meeting global and local slenderness limits; (2) connections, beams and columns are designed to develop the expected tensile, compressive and post-buckling deteriorated resistance of the braces. Brace sizes are determined based on the seismic load combination as specified by ASCE/SEI 7.16, "Minimum Design Loads and Associated Criteria for Buildings and other Structures" [14]. The seismic force-resisting system is designed using two loading conditions: Load State 1 assumes that braces under tensile forces achieve full yielding, while braces under compression forces reach the onset of buckling. In other words, the braces achieve their anticipated strengths. Accordingly, the design horizontal story shear in each bay and story will be less than $(P_{ye} + P_{cre}) \cos\theta$ of the braces, where θ is the angle of the brace with respect to the horizontal axis as seen in Fig 1. Load State 1 results in a larger axial load and smaller bending moment in the beam. Load State 2 assumes that the braces under compression achieve post-buckling strength while the braces in tension yield. Load State 2 results in a smaller axial load and larger bending moment. The expected forces and the resulting beam design forces are illustrated in Fig. 1. Fig. 1a illustrates the resulting beam forces according to the current (i.e. AISC) design. In Fig. 1b, the proposed design is shown where the brace force in tension is assumed to be limited to the brace compressive strength (i.e. $P_{ye} = P_{cre}$). Recent research has indeed demonstrated that the maximum tensile brace force approaches the magnitude of the brace buckling force when weaker chevron beams are used according to the proposed design [5].

In Fig. 1, H_d and V_d are unbalanced horizontal and vertical force demands on the beam, respectively. According the AISC 341-16, the expected strengths for braces are presented in Eq.1 for tension, Eq. 2 and Eq. 3 for compression.

$$P_{ye} = R_y F_y A_g \tag{1}$$

$$P_{cre} = 1.14 F_{cre} A_g \leq P_{ye} \tag{2}$$

$$P_{post-buckling} = 0.3 (1.14 F_{cre} A_g \leq P_{ye}) \tag{3}$$

where A_g is the gross cross-sectional area, $R_y F_y$ is the expected yield strength, and F_{cre} is the expected critical buckling stress. R_y ranges from 1.25 to 1.40 depending on the steel grade and cross section [15]. These equations per AISC 341-16 result in large, unbalanced loads on the chevron beam, which results in deep and heavy beams making the design uneconomical.

Fig. 1b illustrates the unbalanced forces according to the proposed design. Recent large-scale experiments and detailed finite-element analyses have demonstrated that proposed design (i.e. weaker chevron beam) reduces the unbalanced load and provides lateral seismic performance that is comparable with or better than chevron SCBFs designed according to

current requirements [12,13]. This design approach utilizing the beam as an additional yielding element, aligning with previous research on SCBFs which has shown that incorporating extra yielding mechanisms, beyond the brace itself, improves seismic response.

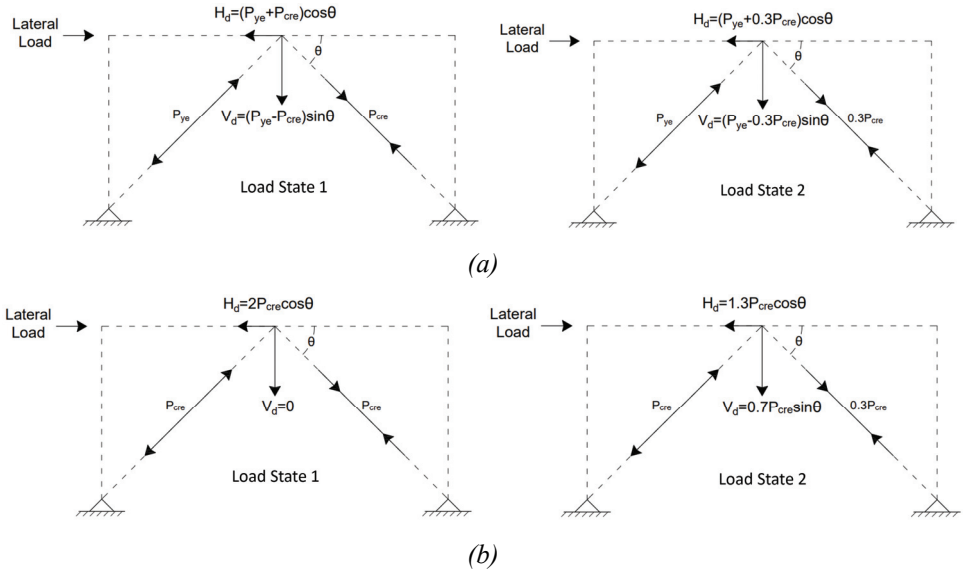

Fig. 1 - Lateral resisting mechanism and the resulting beam forces for Load State 1 and Load State 2 in a chevron-braced frame: (a) AISC, (b) Proposed [5,6].

2.1 Building Model

This study evaluates the seismic performance of 3-story and 9-story prototype buildings with the proposed design by Roeder et al. [5] and Asada et al. [6]. The buildings are designed according to AISC 341-16 “Seismic Provisions for Structural Steel Buildings” [13].

2.1.1. Structural Design

The structural model of the building was developed with the SAP2000 analysis software [16]. It features 7 bays along the X-axis and 3 bays along the Y-axis, each bay spanning 8 meters. The building's lateral resistance system is chevron-braced frames at the perimeter as depicted in Fig. 2a. The structures stand at heights of 12 meters and 36 meters. To support the load, secondary beams are installed at intervals of 2 meters, and a 15-centimeter-thick reinforced concrete slab serves as the diaphragm. Figures 2b and 2c illustrate the elevation views of the 9-story building model. Orgev et al. [17] provide the specifications for the steel profiles used in the model.

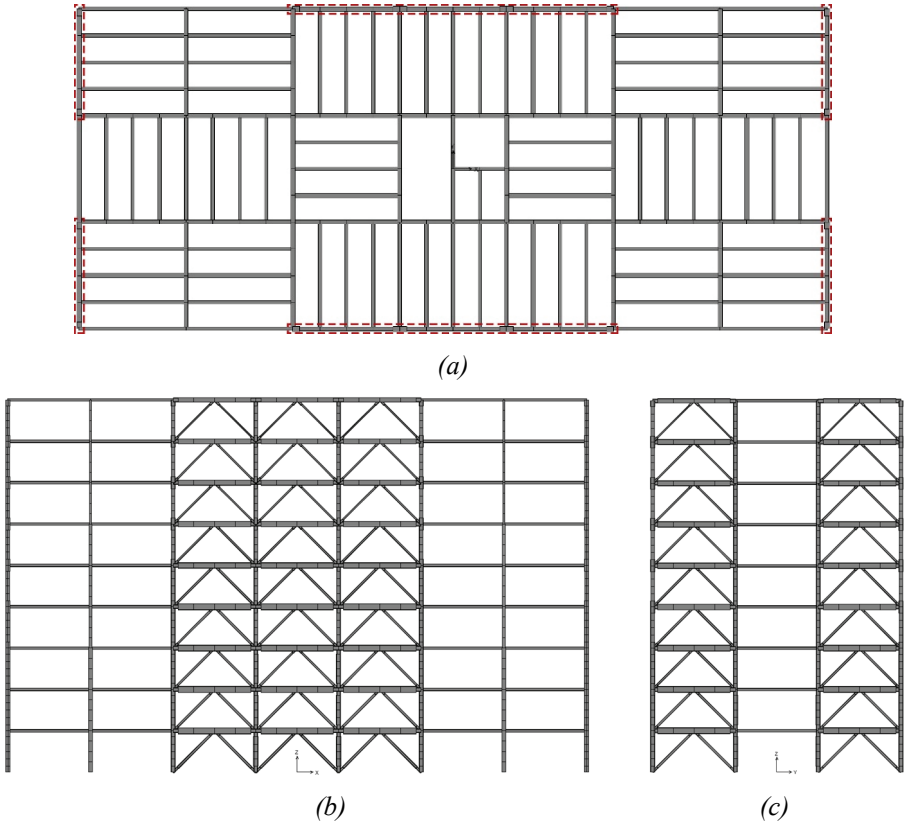

Fig. 2 - Building model: (a) floor plan, elevation view along (b) 9-story X-direction, (c) 9-story Y-direction.

The dead load G is determined as 3.5 kN/m^2 considering both the concrete deck and nonstructural walls. Live load Q is 2 kN/m^2 considering office building occupancy type according to TS498 [18]. The gravity beams are of S275 grade whereas the gravity columns are of S355 grade. The structure is situated in Avcilar, Istanbul, and is classified under soil category ZC. The seismic forces exerted on the building are calculated in compliance with the Turkish Seismic Code [15]. The vertical loading and seismic mass are calculated following the Turkish Seismic Code [15], which considers the contribution of dead loads and a portion of live loads. The seismic mass is determined as G+0.3Q, where G is the total dead load, and 0.3Q represents 30% of the live load. The values for short-period spectral acceleration (S_s) and 1-second spectral acceleration (S_1) are sourced from the Earthquake Hazard Map of Turkey [19]. For soil class ZC, with a shear velocity range of $360 \leq V_{s30} \leq 760$, the design spectra are specified as S_{DS} at 1.5g and S_{D1} at 0.506g. The response spectrum for the site is given in Fig. 3 for Design Earthquake (i.e. 10%/50-year) and Maximum Considered Earthquake (i.e. 2%/50-year). The equivalent seismic force approach is adopted in linear design. The seismic design forces are based on a response modification factor R = 6 according to ASCE/SEI 7.16 [14], which implies a significant ductility. The chevron-braced

frames achieve this ductility because of the capacity-based design per AISC 341-16 [13], where all the supporting members in the lateral force-resisting system (i.e. beams, columns, and connections) are designed to resist the forces resulting from brace buckling and tensile yielding based on the expected yield stress [6]. The importance factor *I* is taken as 1.0. The fundamental periods of the 3-story and 9-story building models are 0.39 s and 1.37 s, respectively for the X-direction; and 0.41 s and 1.39 s, respectively for the Y-direction. Using Turkish Seismic Code (2018), the base shear in Y-direction is estimated as 7058 kN and 6085 kN for the 3-story and 9-story buildings, respectively. Along the Y-direction, there are four chevron-braced frames. Therefore, 3-story and 9-story frames carry 1765 kN and 1521 kN of base shear respectively.

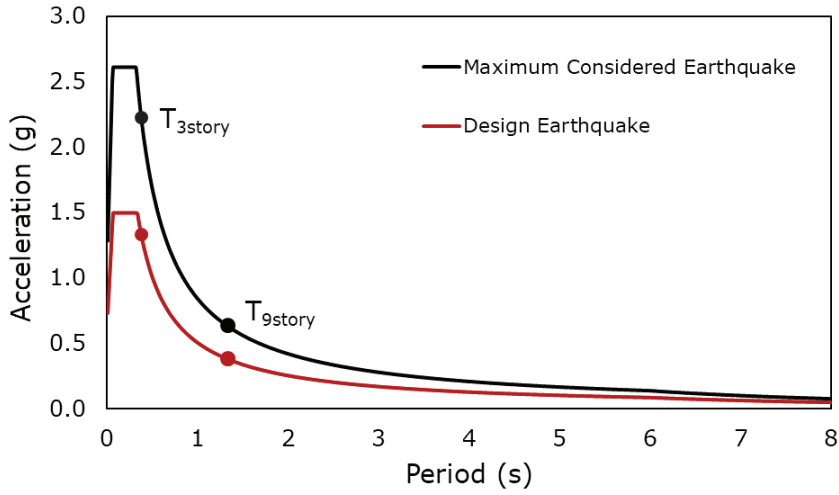

Fig. 3 - Design (10%/50 year) and MCE (2%/50 year) Spectra for 3-story and 9-story buildings.

2.1.2. Nonlinear Analysis and Modeling

A comprehensive model for the nonlinear dynamic analysis is essential to evaluate the performance of chevron-braced buildings. The nonlinear analysis is performed using Perform 3D [7]. The 3-story and 9-story building models are analyzed in 2D (i.e. as planar frames) considering the fundamental period in the critical direction only. The Y-direction is chosen as the critical direction due to its weaker lateral resistance compared to the X-direction. The building models are simplified to 2D representations with a leaning (P-Δ) column to account for gravity columns, as shown in Fig. 4. Considering the 3D model of the building incorporates four chevron-braced frames along the Y-axis, a quarter of the story's mass (and its corresponding weight) is allocated to the leaning column. This is done to simulate the secondary moment impact on the braced frame. An equal displacement constraint is applied between the leaning column and the braced frame at each story level, as illustrated in Fig. 4. The loads corresponding to the effective seismic weight of the tributary area are applied to the nodes, as shown in Fig. 4.

Table 1 lists the chevron-braced frame member sizes for 3-story and 9-story buildings, which are calculated by using the capacity-based method according to AISC 341-16 and according to the proposed design [5,13]. All members are sized such that demand-to-capacity ratios are close to 1 if width-to-thickness ratios are satisfied. The slenderness ratio, denoted as *KL/r*, for the brace members ranges from 50 at the lower floor levels to 100 at the higher floor levels. Two buildings are designed according to current AISC provisions (i.e. AISC) and proposed design (i.e. Proposed). Here, only the chevron beam member sizes are altered. The columns and braces are not modified to isolate the effect of yielding chevron beam on the building seismic performance. In the proposed design, the slenderness ratio of the lower-story braces is reduced by increasing their depth rather than thickness, which raises their moment of inertia without substantially increasing the cross-sectional area. As a result, while the expected tensile strength (P_{ye}) remains largely unchanged, the compressive strength (P_{cre}) increases due to the reduced slenderness ratio. Since the proposed method assumes that the brace force in tension is limited to the brace compressive strength ($P_{ye} = P_{cre}$), the reduced slenderness ratio leads to a smaller unbalanced force on the beam. However, when P_{cre} approaches P_{ye}, the potential for reducing beam sizes diminishes, particularly in the lower stories. Proposed design provides up to 8% less structural weight for each bay compared to AISC design.

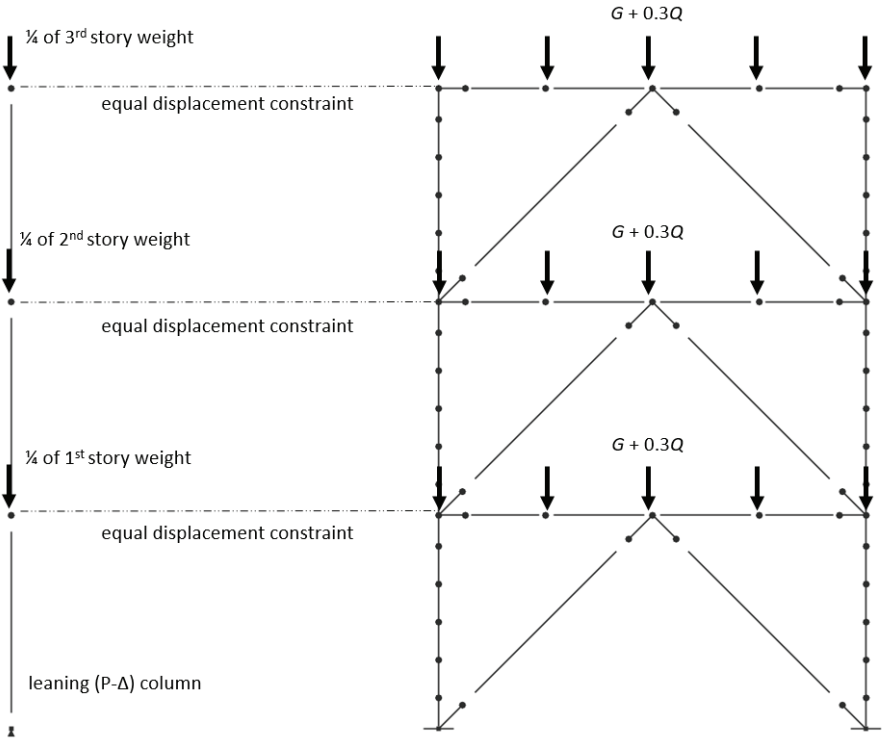

Fig. 4 - Illustration of 2D model for the 3-story chevron-braced building in Perform 3D.

Table 1 - Chevron-braced frame sections for the critical (Y-) direction for building models.

9-story Building									
Story	Brace (S235)	Column (S275)	Beam (S355)		Story	Brace (S235)	Column (S275)	Beam (S355)	
			AISC	Proposed				AISC	Proposed
1	HSS 210x12	HD 400x509	HE600B	HE550B	5	HSS 180x13	HD 400x237	HE550B	HE500B
2	HSS 200x12	HD 400x463	HE600B	HE550B	6	HSS 170x13	HD 400x187	HE550B	HE500B
3	HSS 190x13	HD 400x382	HE600B	HE550B	7	HSS 150x13	HD 400x187	HE500B	HE400B
4	HSS 190x13	HD 400x237	HE600B	HE550B	8	HSS 140x12	HD 400x187	HE500B	HE400B
					9	HSS 120x11	HD 400x187	HE450B	HE300B
3-story Building									
Story	Brace (S235)	Column (S275)	Beam (S355)		Story	Brace (S235)	Column (S275)	Beam (S355)	
			AISC	Proposed				AISC	Proposed
1	HSS 230x13	HD 320x158	HE650B	HE600B	3	HSS 160x12	HD 320x158	HE500B	HE400B
2	HSS 200x13	HD 320x158	HE600B	HE550B					

Fig. 5a shows the nonlinear elements and hinges used in the chevron-braced frame. Inelastic bar element is used for the brace modeling with tension yielding and compression buckling behavior. Rigid elements are used to represent beam-to-column end-zones. To simulate the inelastic response in both columns and beams, the material nonlinearity is idealized through the concentrated plasticity approach using P-M hinges which considers an elliptical axial force-bending moment interaction [7]. The backbone curve parameters of brace elements, PMM hinges at chevron beam ends, at chevron beam midspan and at column-to-beam interface are defined according to ASCE 41-13 [12]. The backbone curve represents the inelastic strength and ductility element behavior including strength loss. Table 2 gives the backbone parameters for chevron beams, columns and braces as determined according to ASCE 41-13 [12]. The yield rotation of beam and column hinges (i.e. θ_y) is allowed to change depending on the axial force on the member. Perform 3D defines an upper and lower limit to change θ_y per ASCE 41-13 [12].

The gusset plates provide rotational restraint at the beam-column regions, which enables the plastic moment development at beam ends [5,6,20]. Hence, the columns shall be designed according to strong column-weak beam principle. The compression backbone parameters are derived through interpolation between the slender and stocky extremes, based on the

slenderness ratio KL/r of the brace members, where the post-buckling brace strength ranges from 30% to 50% of critical buckling strength.

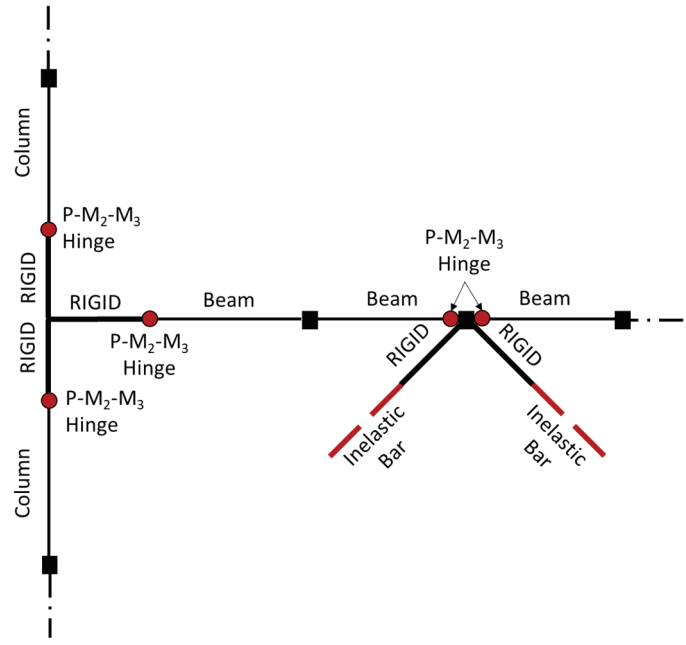

(a)

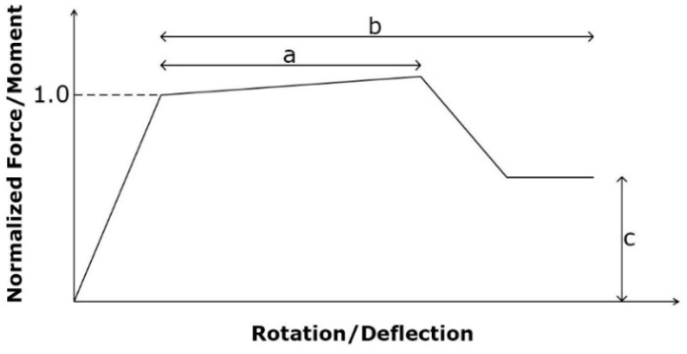

(b)

Fig. 5 – (a) Illustration of nonlinear elements in the chevron-braced frame model, (b) ASCE 41-13 backbone curve [12].

Table 2 - ASCE 41-13 modeling parameters and acceptance criteria for nonlinear procedures of braces, beams and columns [12]. IO: immediate occupancy, LS: life safety, CP: collapse prevention.

Braces (HSS)						
	a	*b*	*c*	*IO*	*LS*	*CP*
Tension	9.0 Δ_T	11.0 Δ_T	0.6	0.5 Δ_T	8.0 Δ_T	11.0 Δ_T
Compression (slender)	0.5 Δ_C	9.0 Δ_C	0.3	0.5 Δ_C	7.0 Δ_C	9.0 Δ_C
Compression (stocky)	1.0 Δ_C	7.0 Δ_C	0.5	0.5 Δ_C	6.0 Δ_C	7.0 Δ_C
Columns						
Tension or Compression	*a*	*b*	*c*	*IO*	*LS*	*CP*
	9.0 θ_y	11.0 θ_y	0.6	1.0 θ_y	9.0 θ_y	11.0 θ_y
Chevron beams						
Flexure	*a*	*b*	*c*	*IO*	*LS*	*CP*
	9.0 θ_y	11.0 θ_y	0.6	1.0 θ_y	9.0 θ_y	11.0 θ_y

The nonlinear pushover analysis of the chevron-braced frame gives the base shear of $V_{3\text{-}story}$ = 4958 kN and $V_{9\text{-}story}$ = 4075 kN according to AISC design. For the Proposed design, the pushover analysis gives the base shear of $V_{3\text{-}story}$ = 4932 kN and $V_{9\text{-}story}$ = 3809 kN according to the Proposed design. Hence, the overstrength value for the 3-story building is Ω = 2.8 for both the AISC and Proposed designs. For the 9-story building, the overstrength values are Ω = 2.7 and Ω = 2.5 for AISC and Proposed design, respectively.

2.1.3. Validation

A single-story chevron-braced frame is validated against a recent experimental program by Roeder et al. [5]. Fig. 6a shows the frame and cyclic loading protocol used in the experiment. The maximum drift used in the protocol prior to brace fracture is 3%. The members are designed according to the provisions of AISC 341-16 [13] except for the beam size. W14x61 (W360x91) beam size is intentionally selected to provide only 55% of chevron-beam resistance by AISC provisions to allow the limited chevron beam yielding mechanism. The material properties of the members used in the braced frame model are taken directly from the experimental program. W14x61 (W360x250) beam is of A992 steel with yield and ultimate strength as 400 MPa and 510 MPa, respectively. W12x50 (W310x74) columns are of A992 steel with yield and ultimate strength as 360 MPa and 450 MPa, respectively. HSS4x4x5/16 (HSS101.6x101.6x7.9) brace is of A1085 steel and has 430 MPa and 515 MPa, respectively. The single-story chevron-braced frame is modeled in Perform 3D according to the ASCE 41-13 modeling parameters and acceptance criteria for nonlinear procedures as shown in Table 2 including the strength loss in tension and post-buckling strength in compression [12]. Fig. 6b shows that the numerical and experimental results of the drift vs.

lateral force (i.e. base shear) prior brace fracture are in good agreement. The model captures the initial stiffness as well as the ultimate strength (i.e. backbone curve) within reasonable accuracy, however the unloading stiffness during cyclic reversal shows some discrepancies when compared to the experiment. The experiment resulted in brace buckling and brace fracture at 0.4% and 3.1% story drift, respectively. The braced frame reached the maximum lateral resistance of 919 kN. This comparison paves the way for using the nonlinear modeling criteria of ASCE 41-13 [12] for braces, beams and other elements, and for creating braced frame building models to conduct nonlinear seismic analyses in accordance with FEMA P695 provisions [11].

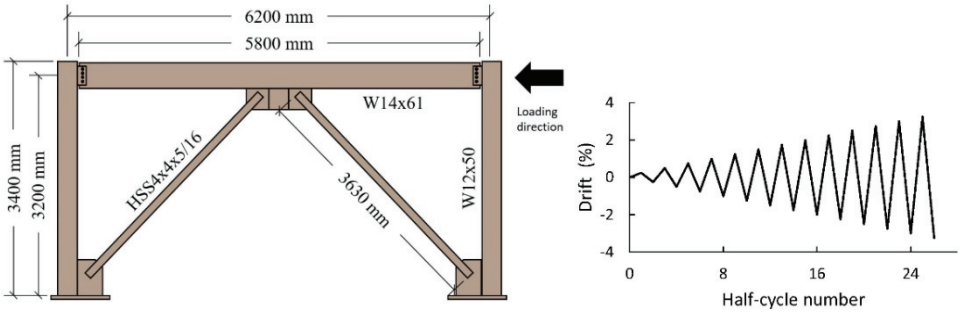

(a) *(b)*

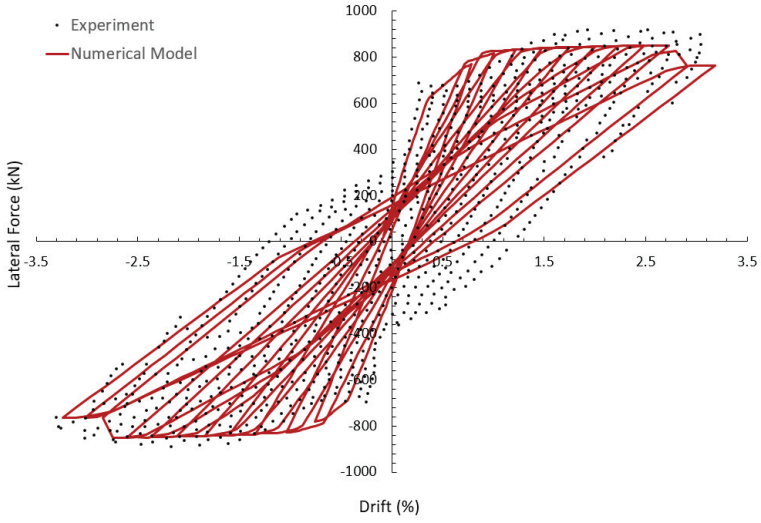

(c)

Fig. 6 - (a) Single story chevron-braced frame used in the experimental test [5], (b) the cyclic loading protocol, (c) validation of the numerical model via base shear vs. drift behavior.

3. NONLINEAR SEISMIC ANALYSIS

To evaluate the seismic performance of 3-story and 9-story chevron-braced steel structures, a risk-targeted methodology involving an incremental dynamic analysis (IDA-based), fragility and hazard curve estimation is employed according to FEMA P695 [11].

3.1 Ground motion selection and scaling

Each building model undergoes a nonlinear time history analysis using 22 pairs of earthquake records from the PEER NGA database [21]. In alignment with the methodology's goals, far-field records with a moment magnitude (M_w) greater than 6.5 are chosen, adhering to FEMA P695 guidelines [11]. The selected records include both strike-slip and reverse faulting earthquakes. The analysis exclusively employs ground motion data recorded on soil classes C and D. The details of the earthquake record set are given in Table 3 and the acceleration-time histories are shown in Fig. 7.

Table 3 - Selected 22 ground motions [21]

PEER ID	Station	M_w	Year	PGV (geomean) cm/s	NF*	**PEER ID**	Station	M_w	Year	PGV (geomean) cm/s	NF*
953	Beverly Hills	6.69	1994	62.9	0.64	**848**	Coolwater	7.28	1992	34.6	1.17
960	Canyon Country	6.69	1994	42.7	0.94	**752**	Capitola	6.93	1989	33.5	1.20
1602	Bolu	7.14	1999	55.9	0.72	**767**	Gilroy Array #3	6.93	1989	40.6	0.99
1787	Hector	7.13	1999	34.1	1.18	**1633**	Abbar	7.37	1990	46.3	0.87
169	Delta	6.53	1979	29.5	1.37	**721**	El Centro Imp. Co.	6.54	1987	44.8	0.90
174	El Centro Array #11	6.53	1979	40.1	1.01	**725**	Poe Road (temp)	6.54	1987	34.5	1.17
1111	Nishi-Akashi	6.9	1995	42.3	0.95	**3744**	Rio Dell Overpass	7.01	1992	57.3	0.70
1116	Shin-Osaka	6.9	1995	26.1	1.54	**1244**	CHY 101	7.62	1999	84.2	0.48
1158	Duzce	7.51	1999	57.2	0.70	**1485**	TCU 045	7.62	1999	48.2	0.84
1148	Arcelik	7.51	1999	23.6	1.71	**68**	LA - Hollywood	6.61	1971	19.2	2.1
900	Yermo Fire Station	7.28	1992	38.6	1.05	**125**	Tolmezzo	6.5	1976	26.4	1.53

* Normalization factor

The ground motion scaling process consists of two steps: (1) Normalizing the geometric mean of peak ground velocities (i.e. PGV) in two directions of each ground motion to the

mean PGV of the record set and (2) scaling each ground motion to the maximum considered earthquake (i.e. MCE) intensity at the corresponding fundamental period $T_{3-story}$ and $T_{9-story}$ of the building models [11]. This two-step scaling process aligns with the ground motion scaling requirements of ASCE 7-16 [14]. The earthquake records are adjusted to the median Peak Ground Velocity (PGV) of the dataset to reduce variations arising from event characteristics like the source type, soil class, and magnitude, ensuring uniformity. The dataset's median PGV is determined to be 40.3 cm/s. It's important to note that this normalization process preserves the integrity of the earthquake events, maintaining the inherent randomness in the records. In the next step, the median value of the normalized record set at the fundamental period $T = 0.41s$ ($S_{median} = 0.84g$) and $T = 1.39s$ ($S_{median} = 0.28g$) are scaled to match the target spectrum demand (i.e. MCE) $S_{MT} = 2.045g$ and $S_{MT} = 0.605g$, respectively. Fig. 8 shows the spectra of 22 ground motion pairs compared to MCE and median spectrum of the record set.

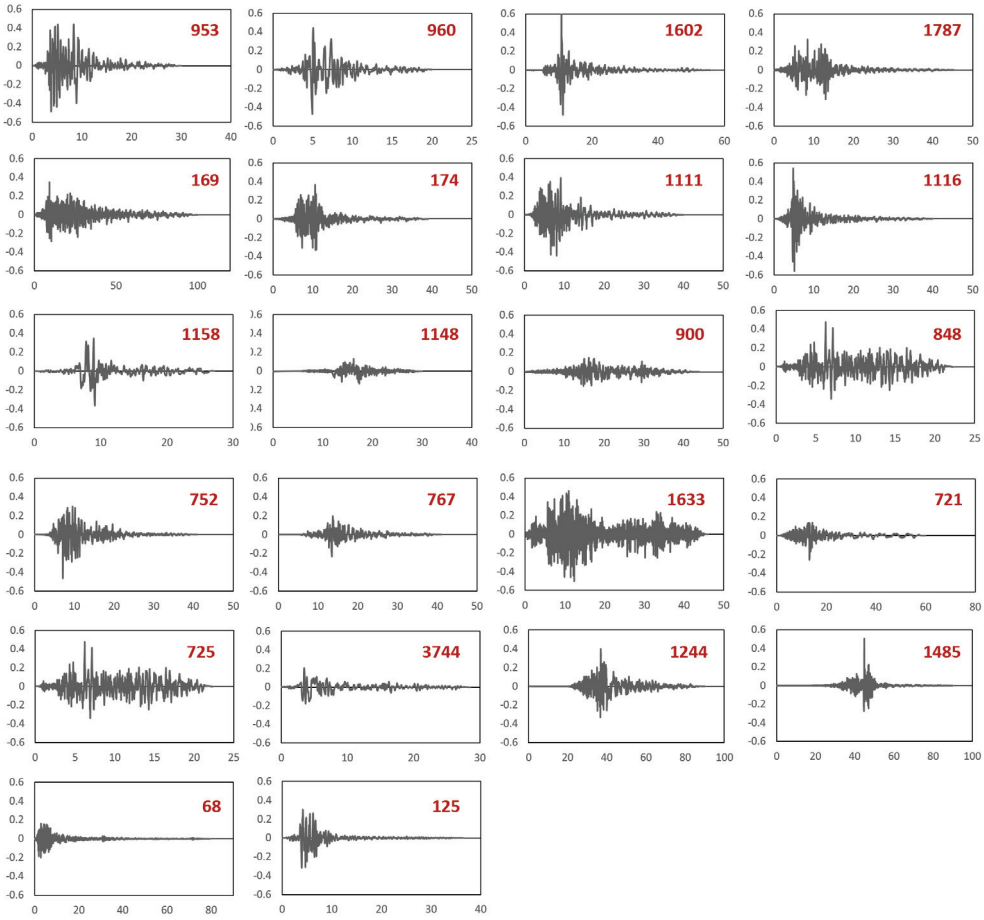

Fig. 7 - Unscaled earthquake record acceleration (g)-time (sec) histories in H2 direction [12].

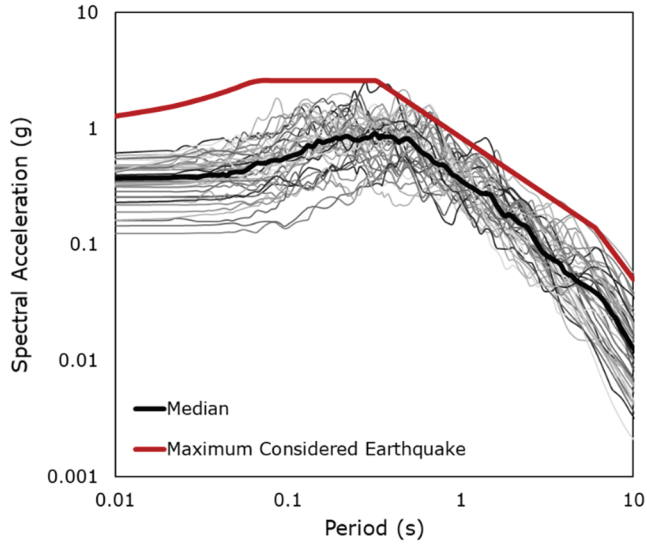

Fig. 8 - Log-log spectral acceleration graph ($\xi = 5\%$) of normalized (unscaled) 22 ground motion pairs including the median of the set and MCE spectrum.

3.2. Local Brace and Beam Response

The local brace and beam responses for the Hector ground motion (as listed in Table 3) are examined by comparing the AISC and Proposed designs. The PMM beam hinge and the brace under investigation are illustrated in Fig. 9a. The plastic rotation time history and the midspan vertical deflection time history of the beam at the intersection of the chevron brace of the 9-story building model are plotted in Fig. 9b and Fig. 9c, respectively. The beam response clearly demonstrates that the Proposed design with smaller beam size (i.e. HEB 300) develops plastic rotation at the chevron brace interaction above the immediate occupancy but below the life safety level according to ASCE 41-13 [12]. The midspan beam deflection history highlights that the secondary yielding beam mechanism is activated in the Proposed design, as anticipated. This mechanism allows the beam to redistribute forces and contribute to energy dissipation, thereby improving overall system resilience. In contrast, the AISC design shows minimal vertical deflection and negligible inelastic deformation. The brace axial force-strain behavior in Fig. 9d indicates that the steel brace undergoes cyclic loading and unloading, which is more pronounced in Proposed design. This represents energy dissipation through inelastic deformations. After the initial cycles, the brace behavior stabilizes at a reduced axial force level, showing that the brace experiences post-buckling behavior, but retains residual strength. Fig. 9e through Fig. 9h illustrate the plastic rotation history of PMM beam hinges on the 7th, 5th, 3rd and 1st floors, respectively. The magnitude of plastic rotation decreases progressively toward the lower floors, indicating reduced inelastic demand at those levels. However, the Proposed design always exhibits greater beam yielding compared to the AISC design.

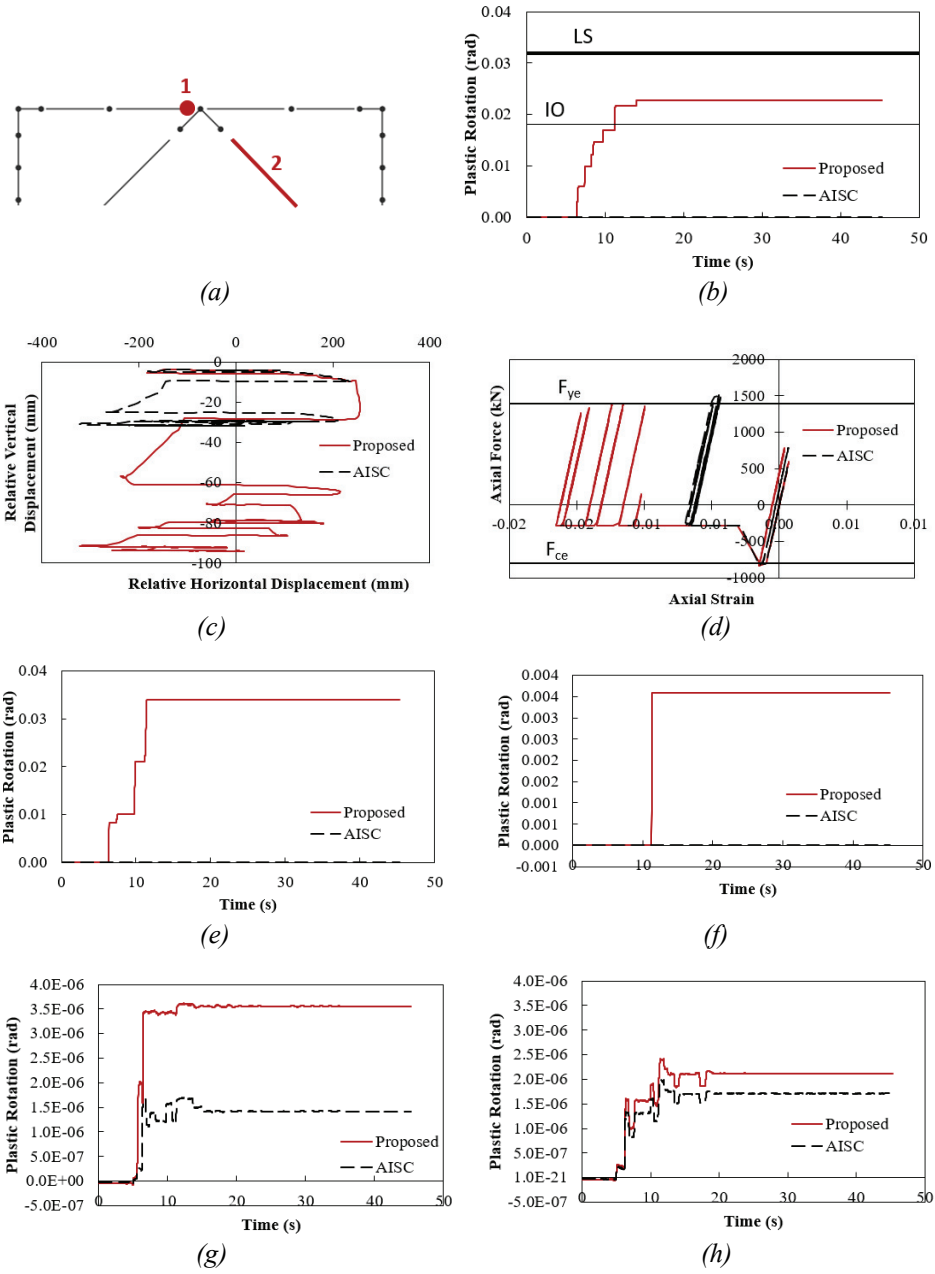

Fig. 9 - (a) The local response locations: PMM hinge on the beam (1) and right brace (2), (b) the plastic rotation history of PMM hinge on 9th story, (c) vertical midspan beam deflection on 9th story, (d) axial strain-force diagram of the brace (F_{ye} and F_{ce}: brace tension and compression capacity) on 9th story, the plastic rotation history of PMM hinge (e) at 7th story, (f) at 5th story, (g) at 3rd story and (h) at 1st story.

3.3. Incremental Dynamic Analysis

Vamvatsikos and Cornell [22] describe collapse as the juncture at which structural analysis fails to converge, leading to instability. Although past studies on gravity frames suggest deformation limits near 8%, concentrically braced frames typically experience strength degradation and brace fracture at much lower drift levels [5,22]. Therefore, an interstory drift ratio of 4% is used to signify the onset of collapse for the structure, as evidenced by the behavior of the Incremental Dynamic Analysis (IDA) curves shown in Fig. 12 and Fig. 13. Around the 4% drift ratio, the curves begin to flatten, implying that the structure is no longer able to sustain increased acceleration demand without a significant increase in deformation. This plateau indicates a loss of stiffness and the start of strength degradation, marking a critical threshold beyond which the structure transitions into an unstable or near-collapse state. The interstory drift ratio is obtained by dividing the relative displacement of two consecutive floors by the story height.

The collapse analysis of the building is initially conducted based on the MCE intensity, which corresponds to a 2% probability of exceedance within a 50-year period. Both 3-story and 9-story chevron-braced building models perform well when subjected to the record sets scaled to the MCE intensity level at their respective fundamental period. The first row of Table 4 shows that ten ground motions scaled to the MCE intensity result in the collapse of the 3-story building model, whereas only two ground motions lead to the collapse of the 9-story building model.

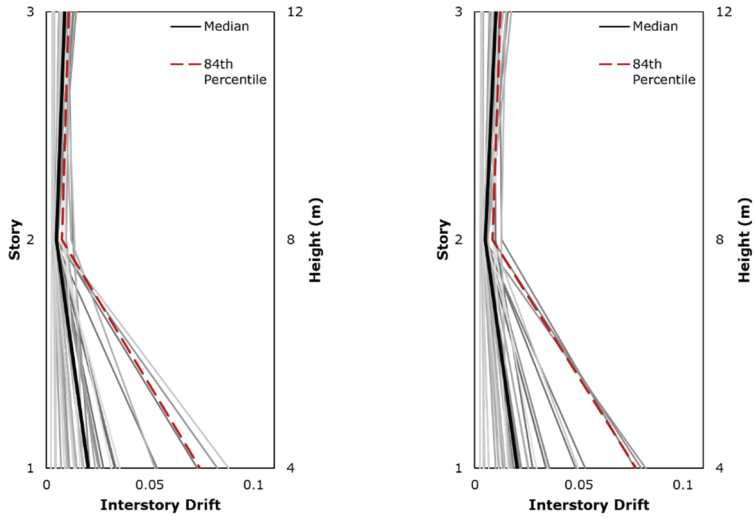

(a) *(b)*

Fig. 10 - Interstory drifts of the 3-story building at MCE intensity designed according to (a) AISC, (b) Proposed

Fig. 10 and Fig. 11 show the interstory drifts of 3-story and 9-story buildings under the MCE spectral intensity, respectively. The interstory drifts along the height of the braced buildings

show similar behavior in both AISC and Proposed design. The maximum value of the median interstory drift remains below 2% and 1% for the 3-story building and 9-story building, respectively. The residual displacements for both designs (i.e. AISC and Proposed) remain below 0.5%, which according to Erochko et al. [23] represents a safe limit for braced steel buildings.

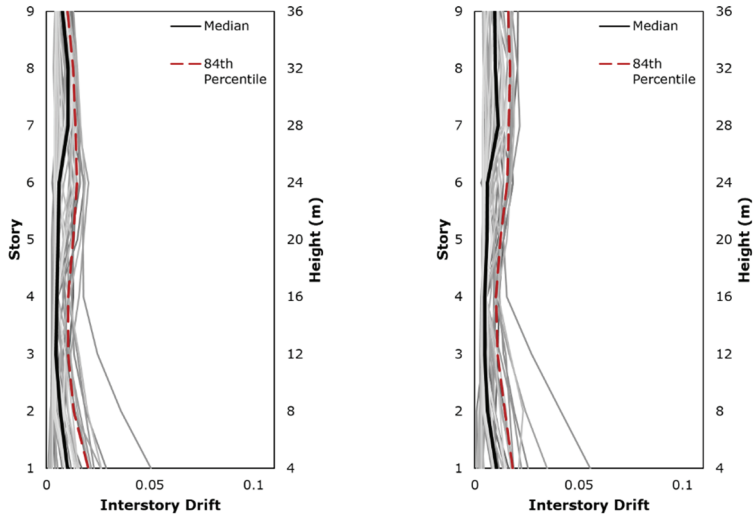

(a) *(b)*

Fig. 11 - Interstory drifts of the 9-story building at MCE intensity designed according to (a) AISC, (b) Proposed.

Table 4 - Summary of incremental dynamic analysis (IDA) for 3-story and 9-story chevron-braced buildings (22 ground motions for each horizontal direction).

3-story building				9-story building			
Scale factor	Spectral acceleration (*g*)	number of collapses (AISC)	number of collapses (Proposed)	Scale factor	Spectral acceleration (*g*)	number of collapses (AISC)	number of collapses (Proposed)
2.43	2.045	10	11	2.12	0.605	2	2
3.16	2.659	15	15	2.76	0.788	6	8
3.60	3.030	22	19	3.43	0.979	18	22
3.74	3.147	23	22	3.73	1.064	22	24
4.37	3.681	29	26	3.90	1.113	25	29
6.08	5.113	39	40	5.30	1.513	42	42
7.29	6.135	44	43	6.36	1.815	43	43

The structural collapse capacity is determined through the use of an incremental dynamic analysis (IDA) approach. In the framework of IDA, the structural nonlinear response-history analyses of 3-story and 9-story chevron-braced buildings is conducted for a set of increasingly scaled earthquake records until the structural collapse occurs (refer to Table 4). The median collapse capacity, denoted as S_{CT}, is the spectral acceleration at which earthquake records are evenly split: half of the records represent instances where the structure withstands the ground motion intensity without collapsing, and the other half represent instances where the structure collapses. The collapse margin ratio, *CMR,* serves as an index of safety against collapse. It is calculated as the ratio of the median collapse capacity, denoted as S_{CT}, to the intensity of the maximum considered earthquake (MCE) ground motion, represented by S_{MT}.

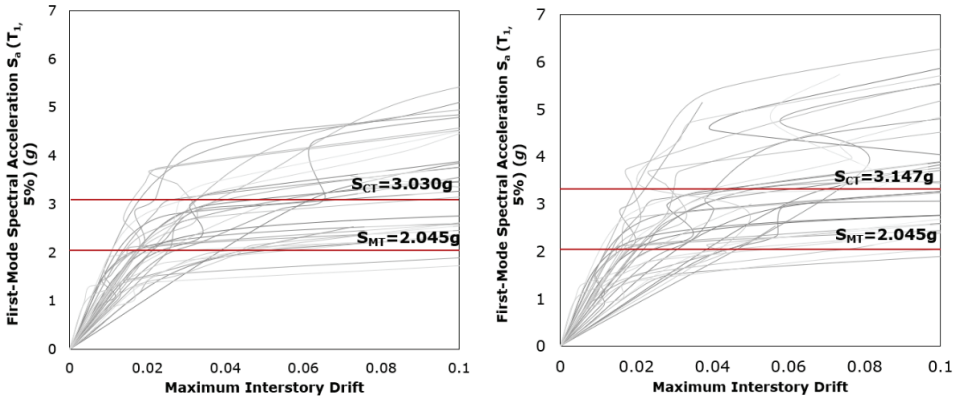

Fig. 12 - IDA results and corresponding S_{CT} and S_{MT} for 3-story building according to (a) AISC, (b) Proposed.

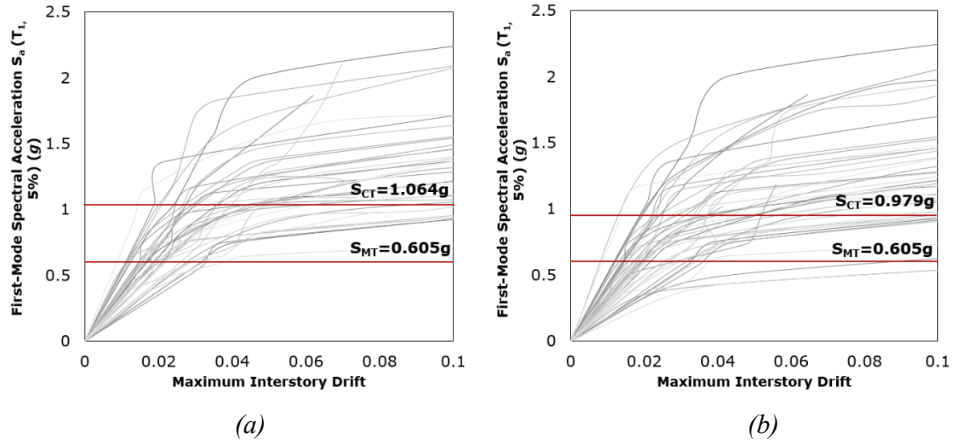

Fig. 13 - IDA results and corresponding S_{CT} and S_{MT} for 9-story building according to (a) AISC, (b) Proposed.

To begin with, each record set is modified with the scaling factor determined in Section 3.1. The scaling factor is used to match the median value of the record set with the MCE spectral intensity S_{MT} at the building's fundamental period. Following this initial adjustment, the scale factor is progressively increased until the point of structural collapse. IDA curves under each earthquake record determine the median collapse capacity, denoted as S_{CT}. The results from IDA analyses are summarized in Table 4. Fig. 12 and Fig. 13 plot the results of IDA in terms of the spectral intensity versus the maximum interstory drift ratio for the 3-story and 9-story buildings, respectively. Each line in IDA curves connects the results for a given ground motion scaled to increasing intensity.

4. FRAGILITY AND HAZARD CURVES

The IDA results establish the collapse capacity for each design variant, which then serves as input to derive fragility curves as outlined in FEMA P695 [11]. The collapse capacity of a structure has various uncertainties arising from ground motion input, structural materials, and construction quality. As defined in FEMA P695 [11], the log-normal cumulative distribution function shown in Eq. 4 is a suitable fragility (i.e. capacity) function to assess the collapse probability of the chevron-braced buildings designed according to AISC and Proposed designs. The fragility curve is defined by the median (θ) and the standard deviation (β). The median gives the intensity for 50% probability of collapse, whereas the standard deviation defines the slope of the fragility curve.

$$F_{capacity} = \frac{1}{2}\left[1 + \mathrm{erf}\left(\frac{\ln x - \theta}{\beta\sqrt{2}}\right)\right] \tag{4}$$

The x-axis of the fragility curve represents spectral acceleration S_a as the intensity measure and the y-axis gives the probability of structural collapse, which was previously defined as 4% maximum interstory drift. To represent the total structural system uncertainty (e.g. numerical modeling and ground motion records), the standard deviation is taken as $\beta = 0.6$ according to FEMA P695 [11]. The median of the fragility curve (θ) is taken as the median collapse capacity (S_{CT}) determined from the incremental dynamic analysis. For the 3-story building, the median collapse capacities are $S_{CT} = 3.030g$ and $S_{CT} = 3.147g$ for AISC and Proposed designs, respectively. For the 9-story building, they are $S_{CT} = 1.064g$ and $S_{CT} = 0.979g$ for AISC and Proposed designs, respectively. The building fragility curves are plotted in Fig. 14. The curves indicate a similar performance of buildings for both designs.

For the risk assessment, a complete form of hazard curve for the building location is required. Hazard curves give the probability of exceeding a certain spectral acceleration for a specific location. By utilizing USGS risk-targeted ground motion calculator [24] and AFAD [19], the hazard curves shown in Fig. 15 are constructed at the fundamental periods of two buildings.

FEMA P695 analysis method for the evaluation of structural collapse is used in this study [11]. In addition, the risk targeted methodology introduced by Luco et al. [25] is utilized to estimate the collapse probability of the buildings in 50 years considering the corresponding hazard curve.

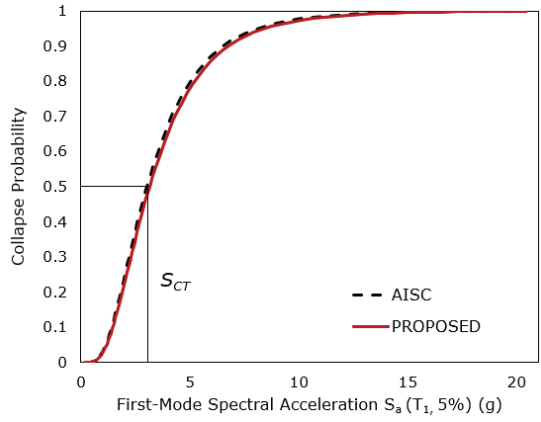

(a)

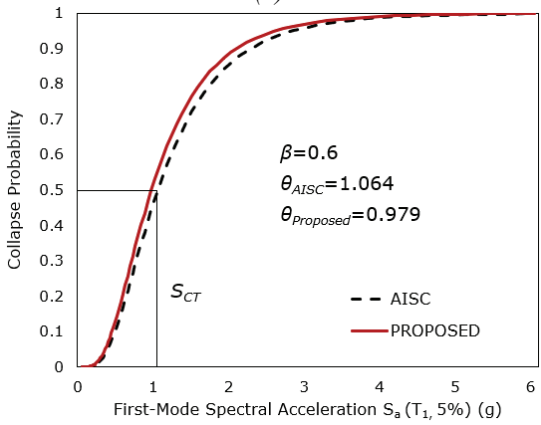

(b)

Fig. 14 - Fragility curves of (a) 3-story and (b) 9-story chevron-braced buildings.

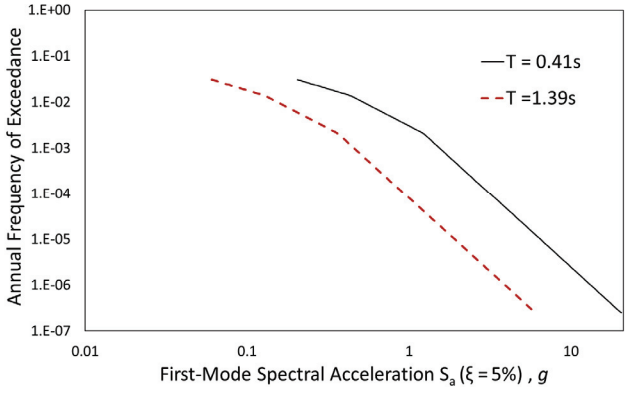

Fig. 15 - Hazard curves for 3-story and 9-story chevron-braced buildings.

5. PERFORMANCE EVALUATION AND SEISMIC RISK ASSESSMENT

The Collapse Margin Ratio (CMR), as defined by FEMA P695 [11], quantifies the structural resilience against collapse. It is determined by the ratio of the median collapse capacity, S_{CT}, to the ground motion intensity of the maximum considered earthquake (MCE) for the 3-story building ($S_{MT} = 2.045g$) and the 9-story building ($S_{MT} = 0.605g$). To consider the frequency content of the earthquake, CMR of 3-story building and 9-story building is multiplied by the spectral shape factor $SSF = 1.20$ and $SSF = 1.40$, respectively [11]. This value depends on both the fundamental period of the building and its period-based ductility μ_T [25]. According to FEMA P695, the period-based ductility is estimated by conducting nonlinear static pushover analyses for the buildings until 20% reduction in base shear is achieved. For 3-story and 9-story buildings, the period-based ductility is $\mu_T = 3.5$ and $\mu_T = 4.5$, respectively. The adjusted collapse margin ratio (*ACMR*) is estimated by the multiplication of *SSF* and *CMR*. For the 3-story building, *ACMR* is 1.78 and 1.85 for AISC and Proposed designs, respectively. For the 9-story building, *ACMR* is 2.46 and 2.27 for AISC and Proposed designs, respectively. There is an improvement in *ACMR* for 3-story building if designed according to Proposed.

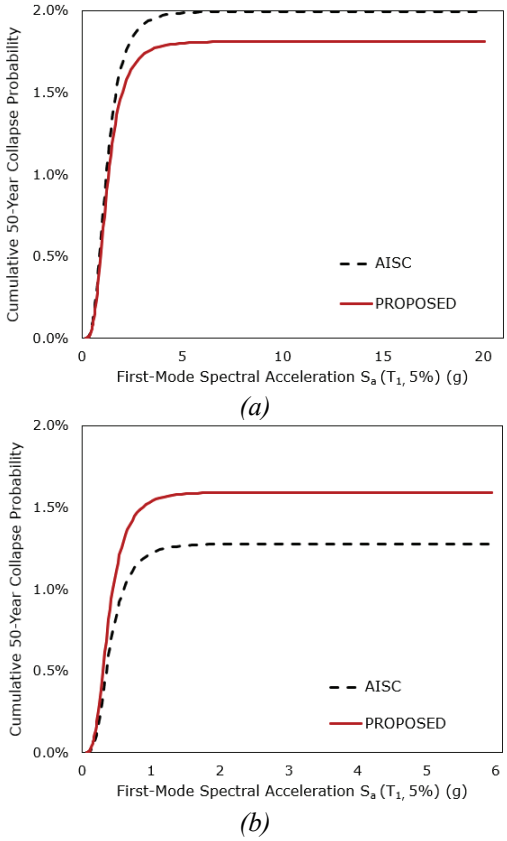

Fig. 16 - 50-year collapse probability curves of (a) 3-story and (b) 9-story chevron-braced buildings.

FEMA P695 method requires an estimate of the system ductility, the structural fundamental period and total system collapse uncertainty to determine an acceptable $ACMR_{20\%}$. ACMR 20% is selected in accordance with the default acceptance criteria outlined in FEMA P695 for evaluating collapse safety under seismic loading. This threshold ensures that the probability of structural collapse at the MCE level does not exceed 20%, which aligns with the risk-targeted performance objectives of modern seismic design codes. It provides a balanced level of safety suitable for typical occupancy structures while allowing for practical and efficient design solutions. Accordingly, for both building models, $ACMR_{20\%}$ shall be at least 1.66 or above according to Table 9-7 in FEMA P695 [11]. All the buildings designed with current AISC and Proposed methods deliver this threshold.

Luca et al. [25] proposed the risk-targeted map to consider both seismicity and building collapse capacity to calculate the structural collapse probability (P_C) in a predefined year t according to Poisson model as in Eq. 5, where λ_C is the mean annual frequency of collapse. In Eq. 6, λ_C is defined as the integral of seismic hazard curve (λ_H) and the slope (i.e. derivative) of building fragility curve ($F_{capacity}$). In most design codes, 1% to 2% collapse probability in 50 years is considered as an acceptable risk [15]. The risk-targeted ground motion calculator created by USGS [24] refers to the methodology of Luco et al. [25] to obtain the risk-targeted ground motion corresponding to a 1% cumulative probability of collapse in 50 years. By utilizing the risk assessment methodology of Luco et al. [25], Fig. 16 shows the cumulative 50-year collapse probability estimates of 3-story and 9-story chevron-braced buildings with AISC and proposed designs. The building collapse risk in 50 years is 2.0% and 1.8% for the 3-story buildings with chevron beams designed according to AISC and proposed method, respectively. The building collapse risk in 50 years is 1.3% and 1.6% for the 9-story buildings with chevron beams designed according to AISC and proposed method, respectively. Table 5 summarizes the performance evaluation results according to FEMA P695 [11] and Luco et al. [25] collapse risk methodologies.

$$P_C(t) = 1 - e^{-\lambda_C t} \tag{5}$$

$$\lambda_C = \int_0^\infty \lambda_H \frac{dF_{capacity}}{dx} dx \tag{6}$$

Table 5 - Performance evaluation results

Structural model	Design method	$\geq ACMR_{20\%} = 1.66$ FEMA P695 [11]	Collapse risk Luco et al. [25]
3-story building	AISC	1.78	2.0%
	Proposed	1.85	1.8%
9-story building	AISC	2.46	1.3%
	Proposed	2.27	1.6%

6. CONCLUSION

This study evaluates the 3-story and 9-story prototype chevron-braced steel buildings with proposed chevron beam yield mechanism. Previous research showed clear experimental evidence of the advantages in using smaller chevron beam sizes. If adopted in design, this will provide a wider applicability for chevron-braced buildings in practice. The novelty of this research lies in two key aspects: (1) the adoption of ASCE 41 modeling parameters and acceptance criteria for nonlinear brace, beam, and column elements in the numerical building models, and (2) the provision of a 50-year collapse risk assessment of the current AISC and Proposed designs, following FEMA P695 seismic provisions and the risk targeted ground motion methodology. Nonlinear time history analyses are performed with 22 ground motion pairs followed by the incremental dynamic analysis. The results show compelling evidence that the proposed design, featuring reduced sized chevron beams, offers similar seismic performance to chevron-braced frames designed according to the AISC provisions. The following conclusions are drawn based on the analysis results of this study:

- The cyclic lateral performance of the chevron-braced frame model using nonlinear modeling criteria of ASCE 41 is validated with experimental results.
- The seismic performance of building models with current AISC and Proposed chevron beams are both found adequate according to FEMA P695 provisions.
- Proposed design provides a more economical solution. Chevron-braced frames with smaller chevron beam have up to 8% less structural weight for each bay compared to the current AISC design.
- For both 3-story and 9-story buildings, AISC and Proposed designs offer satisfactory margin of safety against collapse according to FEMA P695.
- For both 3-story and 9-story buildings, the cumulative collapse risk over 50 years remains within acceptably low limits of 1% to 2% range for both AISC and Proposed designs. However, the variability of collapse risk is smaller for Proposed designs regardless of the building height, compared to the current AISC provisions with heavier chevron beams.

Acknowledgements

The authors also acknowledge UPS Foundation Visiting Professor funding from Stanford University and the assistance of Prof. Gregory Deierlein from Stanford University with literature of steel brace behavior and for the work of graduate student Hava Nur Yavas from Bogazici University.

References

[1] Alqahtani, H., Elgizawi, L.S., The Effect of Openings Ratio and Wall Thickness on Energy Performance in Educational Buildings. Int. J. Low-Carbon Technol., 15(2), 155-163, 2020.

[2] Zheng, L., Dou, S., Zhang, C., Wang, W., Ge, H., Ma, L., Gao, Y., Seismic Performance of Different Chevron Braced Frames. J. Constr. Steel Res., 200, 107680, 2023. https://doi.org/10.1016/j.jcsr.2022.107680

[3] Li, H., Zhang, W., Zeng, L., Seismic Assessment of Chevron Braced Frames with Differently Designed Beams. Struct., 49, 1028-1043, 2023. https://doi.org/10.1016/j.istruc.2023.02.002

[4] Costanzo, S., D'Aniello, M., Landolfo, R., Seismic Design Criteria for Chevron CBFs: European vs North American Codes (Part-1). J. Constr. Steel Res., 135, 83-96, 2017.

[5] Roeder, C.W., Sen, A.D., Terpstra, C., Ibarra, S.M., Liu, R., Lehman, D.E., Berman, J.W., Effect of Beam Yielding on Chevron Braced Frames. J. Constr. Steel Res., 159, 105817, 2019. https://doi.org/10.1016/j.jcsr.2019.04.044

[6] Asada, H., Sen, A.D., Li, T., Berman, J.W., Lehman, D.E., Roeder, C.W., Seismic Performance of Chevron-Configured Special Concentrically Braced Frames with Yielding Beams. Earthquake Eng. Struct. Dyn., 49(15), 1619-1639, 2020. https://doi.org/10.1002/eqe.3320.

[7] CSI, Perform 3D-Nonlinear analysis and performance assessment for 3D structures, User guide, Version 4, Computers and Structures Inc., Berkeley, California, 2006.

[8] Kumar, P.C.A., Sahoo, D.R., Kumar, A., Seismic Response of Concentrically Braced Frames with Staggered Braces in Split-X Configurations. J. Constr. Steel Res., 142, 2018. https://doi.org/10.1016/j.jcsr.2017.12.005

[9] Hassanzadeh, A., Gholizadeh, S., Collapse Performance Aided Design Optimization of Steel Concentrically Braced Frames. Engineering Structures, 197:109411, 2019. https://doi.org/10.1016/j.engstruct.2019.109411

[10] Seker O., Seismic Response of Dual Concentrically Braced Steel Frames with Various Bracing Configurations, J. Construc. Steel Res., 188: 107057, 2022. https://doi.org/10.1016/j.jcsr.2021.107057

[11] FEMA, Quantification of Building Seismic Performance Factors, in: FEMA P695, Federal Emergency Management Agency, Washington, D.C., 2008.

[12] ASCE, Seismic Evaluation and Retrofit of Existing Buildings, in: ASCE/SEI 41-13, American Society of Civil Engineers, Reston, VA, 2014, https://doi.org/10.1061/9780784414248.

[13] AISC, Seismic provisions for structural steel buildings, in: ANSI/AISC 341-16, American Institute of Steel Construction, Chicago, IL, 2017.

[14] ASCE, Minimum Design Loads and Associated Criteria for Buildings and Other Structures, in: ASCE/SEI 7-16, American Society of Civil Engineers, Reston, VA, 2017, https://doi.org/10.1061/9780784414248.

[15] AFAD, Turkish Seismic Code, Specifications for Structures to be Built in Disaster Areas, Disaster and Emergency Management Presidency, Ankara, 2018.

[16] Computers and Structures, Inc. (CSI). SAP2000 Version 23.0.0. Berkeley, California: Computers and Structures, Inc., 2021.

[17] Orgev, A. A., Selamet, S., Vatansever, C., Seismic Performance of Multistory Chevron-braced Steel Structures with Yielding Beams. CE/papers, 6 (3-4), 2238-2243, 2023.

[18] TSE, Design Loads for Buildings, in: TS498, Turkish Standards Institute, Ankara, 1997.

[19] AFAD, Turkish Earthquake Hazard Map, Disaster and Emergency Management Presidency, Ankara, https://tdth.afad.gov.tr/, 2017 (accessed in January 2023).

[20] Costanzo, S., D'Aniello, M., Landolfo, R., The Influence of Moment Resisting Beam-to-Column Connections on Seismic Behavior of Chevron Concentrically Braced Frames, Soil Dyn. Earthquake Eng., 113, 136-147, 2018.

[21] PEER (Pacific Earthquake Engineering Research Center), Next Generation Attenuation-West2, http://ngawest2.berkeley.edu/, 2013 (accessed in January 2023).

[22] Vamvatsikos, D., Cornell, C. A., Incremental Dynamic Analysis, Earthquake Eng. Struct. Dyn., 31(3), 491-514, 2002. https://doi.org/10.1002/eqe.141.

[23] Erochko, J., Christopoulos, C., Tremblay, R., Choi, H., Residual Drift Response of SMRFs and BRB Frames in Steel Buildings Designed According to ASCE 7-05, J. Struct. Eng., 137(5), 589-599, 2011. https://doi.org/10.1061/(ASCE)ST.1943-541X.0000296

[24] USGS (United States Geological Survey), Risk-targeted ground motion calculator, https://earthquake.usgs.gov/designmaps/rtgm/, (accessed in December 2022).

[25] Luco, N., Ellingwood, B. R., Hamburger, R. O., Hooper, J. D., Kimball, J. K., Kircher, C. A., Risk-Targeted Versus Current Seismic Design Maps for the Conterminous United States, 2007.